International Journal of Environmental Science and Technology (2025) 22:3641–3654
https://doi.org/10.1007/s13762-024-06164-9

ORIGINAL PAPER

Comparison of SAR and Optical derived Data used in Forest Cover Detection;PALSAR-FNF vs. ESRI LAND-COVER over North Central Türkiye

A. O. Altunel[1] · **D. A. Çelik**[2]

Received: 18 June 2024 / Revised: 13 October 2024 / Accepted: 28 October 2024 / Published online: 15 November 2024

Abstract
Swiftly and reliably establishing a spatially and geometrically correct land-cover map of any region is rather important in natural resource planning for conservation and utilization. JAXA's PALSAR2/PALSAR/JERS-1 Mosaic and Forest / Non-forest maps, which as the name suggested, have specifically focused on global forest cover since 2007, benefiting from L-band SAR imagery. ESRI Land-cover, on the other hand, owing to exceptional Sentinel-2 imagery, has produced rather detailed land-cover maps including a distinct forest class. In this particular study, coverages of 2017–2020 readied by both institutions, utilizing the aforementioned imageries, were questioned on yearly basis against a rather detailed geodatabase which is still-in-effective use by two of the current regional directorates of forestry, Kastamonu and Sinop in Türkiye, utilizing long adopted accuracy metrics (user, producer and overall accuracies). When all year coverages were concerned, the best overall accuracies were held with 82% in 2017 ESRI land-cover and 83% in 2017 PALSAR-FNF. Both datasets yielded relatively good results in the forest class when user accuracies were investigated. ESRI land-covers managed more than 87% across all four years, while PALSAR-FNFs produced 84.33% in 2020 as the highest scoring year. As for producer accuracies, PALSAR-FNFs produced over 89% across all year coverages, while ESRI produced 84% in 2017 as the highest scoring year. It is worth noting that the ESRI land-covers had better compliance with the compartment boundaries of the reference geodatabase.

Keywords ESRI Land-cover · Sentinel-2 · L-band SAR · PALSAR2/PALSAR/JERS-1 Mosaic FNF Maps

Introduction

Land-cover classification studies have come to everyone's attention in the early 1970s after the Earth Resource Technology Satellite (Landsat-1) was launched in July 1972 and started collecting imagery from all over the Earth. Imagery acquired by the satellite was used in devising the first study of the normalized difference vegetation index (NDVI), which is now a ubiquitous indicator of global plant health (Rouse et al. 1974). Land-cover is both an essential information for various applications concerning Earth dynamics e.g. forests, agricultural fields, glaciers, water, man-made objects, carbon etc. (Kucsicsa and Balteanu 2020; Altunel and Kara 2023; Celik and Sahin 2023), how they are changing over time (Skalos et al. 2012; Zhu et al. 2022) and what will be an effective solution to capture the detail (Karakus et al. 2017). How they are utilized (land use) and how this usage is altered by human-induced processes (land change), can also be monitored (Liping et al. 2018; Kaptan et al. 2022). Thus, a number of natural and human-triggered phenomenon, such as climate change (Jiang et al. 2018) natural forest loss (Galiatsatos et al. 2020), urbanization (Lopez et al. 2017) and land-mass movements (Wang et al. 2022; Altunel, 2023) etc. can better be explained in different scales. Led by Landsat, medium resolution satellite data, e.g. SPOT, IRS, JERS-1, PALSAR have extensively been used to map land-cover in various scales. They have been considered as the foundation in sustainable management of precious resources, forests at the forefront (Dibs et al. 2023b). When technology

Editorial responsibility: S. Mirkia.

A. O. Altunel
aoaltunel@kastamonu.edu.tr

D. A. Çelik
dcelik@kastamonu.edu.tr

[1] Forest Engineering, Faculty of Forestry, Kastamonu University, Kastamonu, Türkiye

[2] Forestry, Arac Vocational School, Kastamonu University, Arac, Kastamonu, Türkiye

has enabled us to improve the image resolution further, the results that were reached using these new data, have started coming up with much better definitions and precisions (Dibs et al 2023a).

Although impressive ground sampling achievements are available for multitude of occasions today (Kwan et al. 2017; Nkeumoe Numbisi et al. 2018) long-time, archive-building, image acquisition which has led to globally oriented land-cover change detection studies focusing primarily on forests has only been possible with Landsat (Townshend et al. 2012; Hansen et al. 2013) and JAXA missions (Shimada et al. 2014) because only a handful of missions were extensive and long-lasting enough for the task (Wulder and Masek 2012; Lulla et al. 2021). Garcia-Alvarez and Hinojosa (2022) disclosed all thematic land-cover datasets, however rather credible additional ones have started appearing in portals, thanks to new imageries and algorithms. Majority of them lack sequential coverages, and the interest on how effective those really are in the long run, is rather limited (Akturk et al. 2023).

Two of such global datasets released with a number of sequential year coverages, have been 10 m ESRI Land-cover maps (ESRI coverages) and 25 m Japan Aerospace Exploration Agency (JAXA) Global PALSAR-2/PALSAR/JERS-1 Mosaic and Forest / Non-forest Maps (PALSAR-FNF coverages). L-band SAR data also proved its usefulness in numerous occasions (Li et al. 2022; Garg et al. 2022; Koyama et al. 2022). Image classification algorithms vary considerably (Chen et al. 2021; Wang et al. 2022; Aksoy and Kaptan 2022). The imagery used in the making of PALSAR and ESRI coverages have been effectively produced successful results in numerous occasions (Comert et al. 2019; Zhang et al. 2018). Each source data has independently (Leenstra et al. 2021) and complementarily been used in various studies (Roy et al. 2019). The established models were validated through seasonally dated imagery captured throughout the year in question (Pastick et al. 2018) and approved outputs were combined in a final year representing coverage. Although both could be considered as medium resolution for land-cover studies, it was obvious that Sentinel-2 based ESRI land-covers would have an edge in class definitions. Deep learning methodology was the method of choice when composing the ERSI coverages finalized using 4, 10 m bands of Sentinel-2 surface reflectance data composed of blue, green, red, near-infrared and two additional 20 m short-wave infrared bands (Cazaubiel et al. 2017; Karra et al. 2021). Whereas, random forest methodology in PALSAR-2 coverages composed using 25 m L-band SAR imagery (Shimada et al. 2014) were employed in the making of the released year coverages between 2017 and 2020.

As a relatively late comer in this arena, European Space Agency's (ESA), Copernicus Sentinel-2 twin satellites, Sentinel-2A and -2B swiftly amassed enough data since 2A's launch in June 2015. Higher-resolution Sentinel-2 imagery have proven itself on each occasion, obvious from various studies (Iurist et al. 2016; Main-Korn et al. 2017; Phiri et al. 2020; Kluczek et al. 2022). Five new 10 m Global land-cover maps (2017, 2018, 2019, 2020 and 2021) built using Sentinel-2 archive imagery were released by ESRI on July 2021. Similarly, the exact same year PALSAR-FNF coverages being released by JAXA since January 2014, created perfect opportunity to assess the weak and strong points of both datasets.

This study was devised to see how the sensitivities of both ESRI and PALSAR-FNF coverages focusing on whatever classes were identifiable within the study area, would compare against the currently in-effective-use, field verified forest management oriented geodatabase stretched over a rather extensive geographical region in North-Central Türkiye.

Materials and methods

Study area

The study area includes two heavily forested provinces, Kastamonu (KRDF) and Sinop (SRDF) (Fig. 1), which since 2022 have become two independent regional directorates of forestry. The data that we used in this study was from the former Kastamonu regional directorate of forestry (KRDF) database that had included these two provinces before 2022. As of 2020, they boasted a combined acreage of almost 1,893,665.54 ha both predominantly fully and partially closed forest area with 1,270,360 m^3 annual increment. Positioned side by side over the central Black-sea coast of Türkiye, the area is prime forest growing part of the country. Sea warmed air coming from the North dumps lots of precipitation varying in composition throughout any given year (Atalay and Efe 2010; Celik et al. 2012) not only to the area, but also to all across the Black-sea region.

Although professionally managed by the forest service since 1963, the first-ever digitally conceptualized forest management planning in Türkiye as mandated by the forest service, started to be enforced in 2008 (Baskent et al. 2008). KRDF managed to adopt this mandate in 2012–2014 period, establishing a comprehensive forest management perspective across its administrative extent in vector format. One of the main purposes of this study was to show that these datasets, ESRI land-cover and PALSAR-FNF prepared around the World may have discrepancies in Türkiye or elsewhere. The most important criterion in choosing the area for this study is that Kastamo-Sinop region has the highest area ratio in terms of forest area, around 67%, the industrialization and

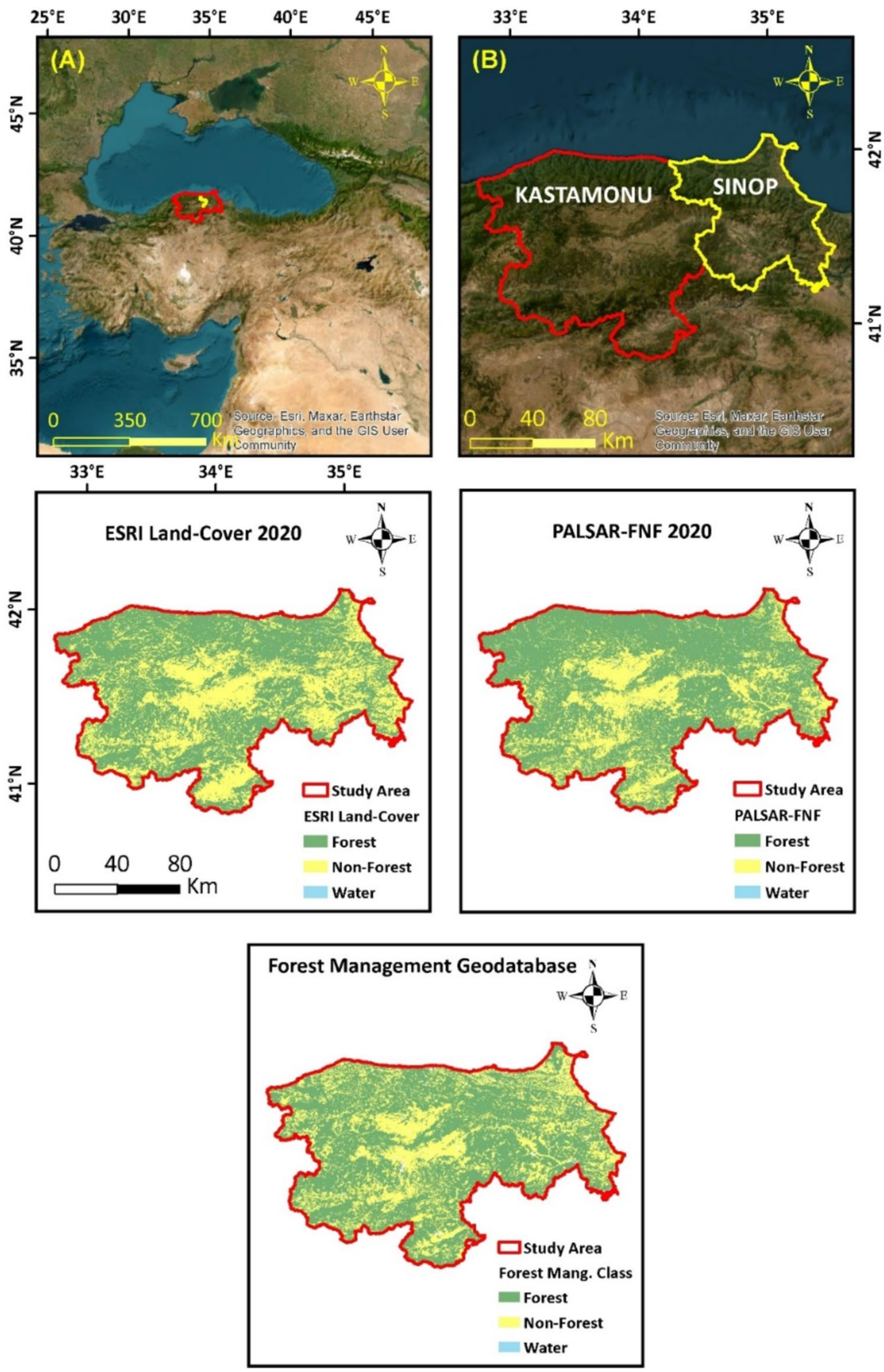

Fig. 1 **A** Türkiye extent of the study area, **B** two provinces making up the former KRDF, followed by the respective vectorized comparison and validation datasets

the urban encroachment densities were below average, and it ranked first in terms of timber production.

Methodology

Validation dataset

Although intended and produced for forestry purposes, KRDF regional forest management plan (geodatabase) included major land-cover land-use classes, forest, agriculture, urban, scrub/shrub, rangeland, and bare ground and water. KRDF forest management plan (1,893,665.54 ha) encompassing 182 individual planning units, which are current to sub-compartment level, is used as field validation dataset in this study (Fig. 1). Forest management maps and field study reports used in Turkish Forest Service, are prepared based on the principles specified in forest management guidelines (URL-3, 2017). In this particular study in which 2014-finalized such forest management geodatabase (tree or mixture specific sub-compartment level precision) was used. It was the culmination long lasting forest inventories, in which crews had always gathered field samples from 400, 600 and 800 m^2 circular plots corresponding to the nodes of systematically placed 300 m × 300 m grid. Crown closure was the decisive factor in deciding the sampling plot size. Simultaneously or previously gathered high resolution stereo air photos and satellite imagery had also been used as supplementary data while finalizing the timber cruising reports eventually making the entire geodatabase. Thus, national forest acreage and volume amounts have been meticulously recorded and tabulated since the 1960s (URL-4, 2019).

Sub-compartments housing the mature age classes were excluded fearing the possibility of unfair mismatch due to final harvests occurring in any of the questioned years. Thus, a mask layer composed of these excluded sub-compartments was applied to all year coverages before calculating the acreages. Each year's Google Earth imagery was also used to further rectify the KRDF geodatabase to better form a year corresponding updated validation dataset.

ESRI Land-cover datasets

Global ESRI Land-cover coverages, 2017–2020 produced utilizing the success culminated by Sentinel-2 mission and the similarly intended corresponding years' PALSAR-FNF coverages by JAXA were compared against the mentioned regional forest management geodatabase of KRDF (pre-2022 extent).

2021 ESRI coverage was not evaluated simple because the corresponding year's PALSAR-FNF coverage was not ready. ESRI released these maps as grab and go in July 2021. They were materialized by high-resolution Sentinel-2 imagery and produced employing a machine learning methodology. Time correct and comparable year compilations were used to materialize each year's coverages with 9 classes. Such successional maps are enjoyed by many for monitoring the effects of land-cover changes in the long run, the increase or decrease of surface water capacities (Ohki et al. 2019), the food production projections (Lambert et al. 2018) and sustainable management of natural ecosystem services (Vaz et al. 2019; Loran et al. 2018), but the studies have mostly been limited to the case (Isaienkov et al. 2020), area (Watanabe et al. 2016) or the region (Camalan, 2022) because of the lack of abled datasets or processing capabilities in many parts of the Earth. Although categorized as mature after March, 2022, still accessible ESRI coverages pertaining to the above mentioned years have come with the following class definitions starting with 1 as Water, 2 as Trees (natural or plantation forests and alike), 3 as Flooded vegetation, 4 as Crops (Agriculture), 5 as Rangeland (Scrub/Shrub), 6 as Build area (all sorts of human intervention), 7 as Bare ground, 8 as Snow/Ice and 9 Clouds. Land-cover data for 2017–2020 was downloaded from the ESRI portal by using a 10 km buffer zone to avoid data loss in the study area (URL-1, 2023; Altunel and Çelik, 2023). Afterwards, we consolidated classes 3, 4, 5, 6, 7, 8 and 9 into non-forest and kept remaining 2 classes as were.

PALSAR-FNF datasets

PALSAR-FNF coverages, on the other hand, have readily been available to the end users since January 2014. They have provided yearly coverages in two periods; 2007 to 2010 and 2015 to 2022. Random-forest algorithm was preferred in their making. They have contained 4 classes, 4th being no-data. Although limited in the number of classes compared to those of ESRI coverages, they, too, were easily definable across the corresponding year coverages; 1 as Forest (more than 10% canopy cover), 2 as Non-forest (everything is included except the first class), 3 as Water and 4 as no-data or unclassified (Shimada et al. 2014). As opposed to Sentinel-2's multispectral imagery, PALSAR-FNF coverages were produced by assembling long paths of L-band Synthetic Aperture Radar (PALSAR) backscatter images observed through JAXA's global Basic Observation Scenario for PALSAR on Advanced Land Observing Satellite (ALOS). 9 separate PALSAR-FNF tiles per year, were downloaded to cover the study area (URL-2, 2023). Since PALSAR-FNF's classification was rather limited compared to that of ESRI land-cover, we adopted a simpler approach to make ESRI land-cover to appear like PASAR-FNF. Thus, three final classes, forest, non-forest and water were aggregated.

All three datasets, one field verified GIS geodatabase and two comparisons, were reclassed to increase the success of the study, and three common classes were adopted as followed; 1 as Forest (all forest defined places in both ESRI and PALSAR-FNF), 2 as Non-Forest (flooded vegetation, crops, rangeland, build area, bare ground, snow/Ice and clouds in ESRI, and non-forest, no-data or unclassified in PALSAR-FNF), 3 as Water (water class of both coverages) (Fig. 2). Both ESRI land-cover and PALSAR-FNF coverages were reprojected to Universal Transverse Mercator (UTM) projection on zone 36 over the horizontal European datum-1950 (UTM-ED50) to coincide with

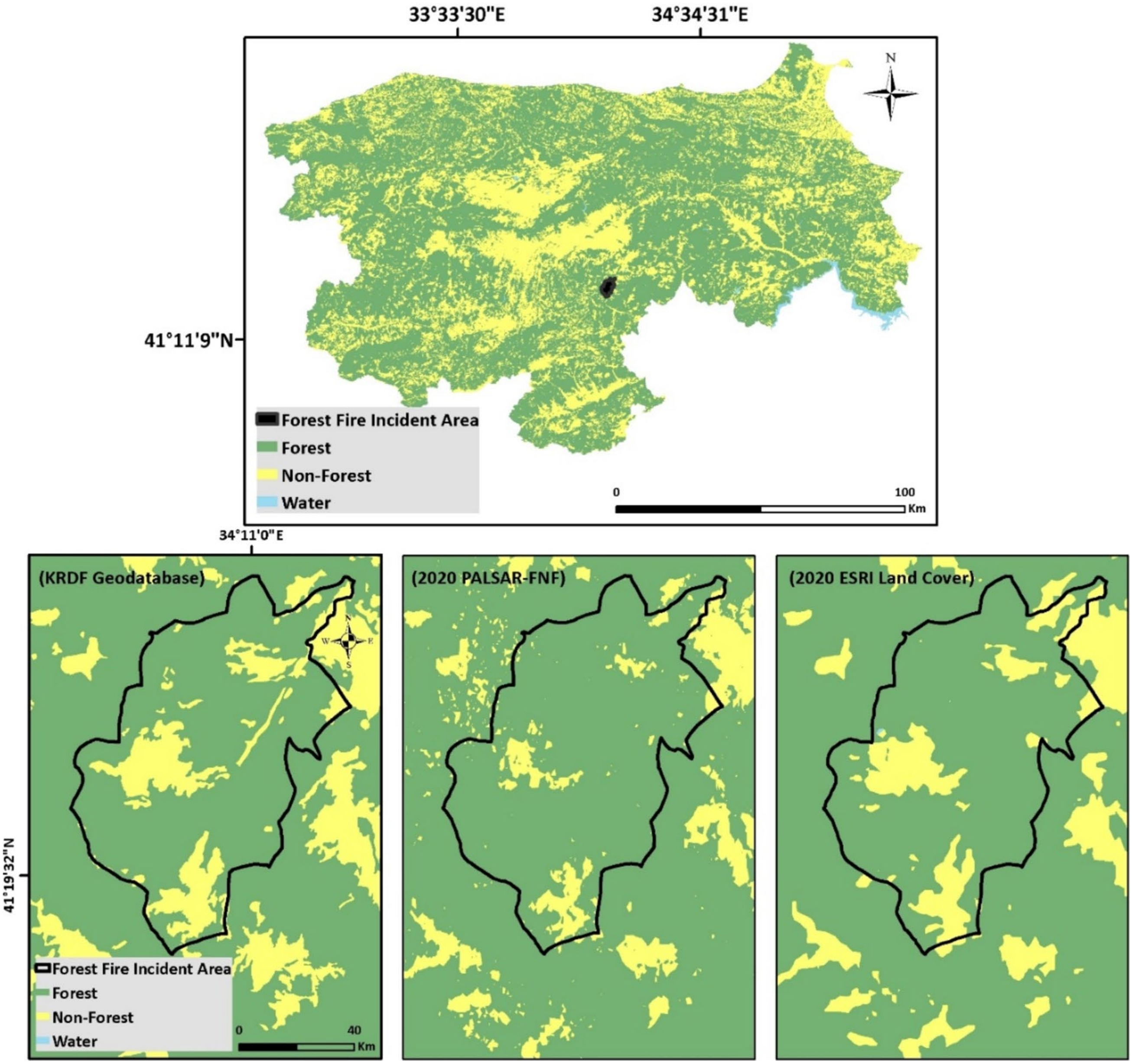

Fig. 2 The affected area of September 2020 fire incident within the study area

the already projected and maintained KRDF geodatabase. The utilized land classes covered large and wide surfaces, and there were no substantial differences over the years. ESRI and Palsar land classes used in the research area were land-cover maps created by certain methods and algorithms over the images collected by passive and active satellite sensors obtained within the particular year. In this study, land-cover maps published by data providers over the years (2017–2020) were compared. Since both databases used the same year images in building the respected year coverages, there was no temporal difference between the datasets.

Finally, both ESRI Land-cover and PALSAR-FNF coverages were subjected to raster to vector conversion to precisely coincide and intersect with the KRDF geodatabase sub-compartment polygons. ArcGIS 10.8 was used in all phases of the study.

Accuracy evaluation

We checked the user (Eq. 1), producer (Eg. 2) and overall (Eq. 3) accuracies based on the acreages resulting from intersections between KRDF geodatabase and yearly-vectorized two comparisons. Accuracy metrics as developed and adopted by many previous studies (Congalton 1991; Campbell, 1996; Campbell and Wynne 2011; Bharatkar and Patel 2013; Congalton and Green 2019; Stehman and Foody 2019) highlighted insight experienced over the coverages (Table 1).

$$UA = \frac{Lc_{ii}}{Lc_{i+}} * 100 \tag{1}$$

$$PA = Lc_{jj}/Lc_{+j} * 100 \tag{2}$$

$$OA = \frac{\sum_{i=1}^{c} Lc_{ii}}{M} * 100 \tag{3}$$

Results

We questioned the spatial accuracies of four-consecutive-year land-cover coverages, 2017, 2018, 2019 and 2020, as produced by ERSI using 10 m Sentinel-2, and by JAXA using 25 m L-band SAR images. Detailed, still in effect, forest management geodatabase was used for field validation.

ESRI Land-cover evaluation

The overall accuracy rate across the years studied was no less than 80%, with the best being 81.54% in 2017, taking all years' coverages into account. As for user accuracies,

Table 1 Three-class classification matrix, where c was the class ranging from 1 to 3. The lines (i) represented the reference, 2014 KRDF geodatabase's classes, and the columns (j) represented yearly-vectorized two comparisons' consolidated classes. Line (Lci +) and column (Lc + j) represented intermediary totals use in the accuracy calculations and M was the total area

Reference Data Classified Comparison	1(Forest)	2(Non-Forest)	3(Water)	Total	User accuracy
1	Lc_{11}	Lc_{12}	Lc_{13}	Lc_{1+}	Lc_{11}/Lc_{1+}
2	Lc_{21}	Lc_{22}	Lc_{23}	Lc_{2+}	Lc_{22}/Lc_{2+}
3	Lc_{31}	Lc_{32}	Lc_{33}	Lc_{3+}	Lc_{33}/Lc_{3+}
Total	Lc_{+1}	Lc_{+2}	Lc_{+3}	M	
Producer accuracy	Lc_{11}/Lc_{+1}	Lc_{22}/Lc_{+2}	Lc_{33}/Lc_{+3}		OA

Table 2 ESRI Land-cover 2017 coverage versus KRDF geodatabase (former extent)

FM 2014 (ha)						
ESRI Land-cover 2017 (ha)		Forest	Non-Forest	Water	Total	User accuracy (%)
	Forest	1,040,362	146,986.3	332.65	1,187,681	87.6
	Non-Forest	197,336.1	495,842.5	2202.18	695,381	71.31
	Water	1042.73	1582.23	7978.74	10,603.7	75.24
	Total	1,238,741	644,411	10,513.6	1,893,666	
Producer accuracy (%)		84	76.9	75.9		OA: 81.54

Table 3 ESRI Land-cover 2018 coverage versus KRDF geodatabase (former extent)

FM 2014 (ha)						
ESRI Land-cover 2018 (ha)		Forest	Non-Forest	Water	Total	User accuracy (%)
	Forest	1,007,446	140,023.2	304.18	1,147,773	87.77
	Non-Forest	230,393.6	502,954	2494.29	735,842	68.35
	Water	901.75	1433.82	7715.11	10,050.7	76.76
	Total	1,238,741	644,411	10,513.6	1,893,666	
Producer accuracy (%)		81.3	78	73.4		OA: 80.16

Table 4 ESRI Land-cover 2019 coverage versus KRDF geodatabase (former extent)

FM 2014 (ha)						
ESRI Land-cover 2019 (ha)		Forest	Non-Forest	Water	Total	User accuracy (%)
	Forest	1,013,313	144,834.3	352.55	1,158,500	87.47
	Non-Forest	224,563.5	498,119.3	2622.42	725,305	68.68
	Water	864.87	1457.43	7538.6	9860.9	76.45
	Total	1,238,741	644,411	10,513.6	1,893,666	
Producer accuracy (%)		81.8	77.3	71.7		OA: 80.21

Table 5 ESRI Land-cover 2020 coverage versus KRDF geodatabase (former extent)

FM 2014 (ha)						
ESRI Land-cover 2020 (ha)		Forest	Non-Forest	Water	Total	User accuracy (%)
	Forest	1,002,063	137,631.8	324.76	1,140,019	87.9
	Non-Forest	235,886.6	505,480.4	3040.03	744,407	67.9
	Water	791.58	1298.79	7148.78	9239.15	77.37
	Total	1,238,741	644,411	10,513.6	1,893,666	
Producer accuracy (%)		80.9	78.4	68		OA: 79.99

Table 6 PALSAR-FNF 2017 coverage versus KRDF geodatabase (former extent)

FM 2014 (ha)						
PALSAR-FNF 2017 (ha)		Forest	Non-Forest	Water	Total	User accuracy (%)
	Forest	1,150,392	222,460.7	401.06	1,373,253	83.77
	Non-Forest	84,690	416,437.8	4194.24	505,322	82.41
	Water	3659.38	5512.49	5918.27	15,090.1	39.219
	Total	1,238,741	644,411	10,513.6	1,893,666	
Producer accuracy (%)		92.9	64.6	56.3		OA: 83.05

Table 7 PALSAR-FNF 2018 coverage versus KRDF geodatabase (former extent)

FM 2014 (ha)						
PALSAR-FNF 2018 (ha)		Forest	Non-Forest	Water	Total	User accuracy (%)
	Forest	1,145,164	233,698.2	398.52	1,379,261	83.03
	Non-Forest	89,920.81	405,201.7	4196.82	499,319	81.15
	Water	3655.7	5511.14	5918.23	15,085.1	39.232
	Total	1,238,741	644,411	10,513.6	1,893,666	
Producer accuracy (%)		92.4	62.9	56.3		OA: 82.18

the highest one was calculated in the forest class, resulting more than 87% in all ESRI yearly coverages, from 87.47% to 87.9%, followed by water class between 75.24% and 77.37% and non-forest class between 68.35% and 77.37%. Producer's accuracies, on the other hand, generated lower figures placing the forest class into the lead with more than 80% in all year coverages, 80.9% to 84%, followed by non-forest class between 76.9% and 78.4%, and water class between 68% and 75.9% (Tables 2, 3, 4 and 5).

PALSAR-FNF evaluation

sWhen PALSAR-FNF yearly coverages were investigated, overall accuracies produced somewhat better results ranging from 83.05 to 81.51% in the rest compared to those of ESRI yearly coverages. While user accuracies resulted between 83.03% in 2018 and 84.31% in 2020 in forest class, 76.23% in 2020 and 82.41% in 2017 in non-forest class and 39.217% in 2020 and 39.232% in 2018 water class in all years (Tables 6, 7, 8 and 9). This poor performance was

Table 8 PALSAR-FNF 2019 coverage versus KRDF geodatabase (former extent)

FM 2014 (ha)						
PALSAR-FNF 2019 (ha)		Forest	Non-Forest	Water	Total	User accuracy (%)
	Forest	1,145,194	229,249.1	432.72	1,374,876	83.29
	Non-Forest	89,888.55	409,652.3	4162.44	503,703	81.33
	Water	3658.04	5509.64	5918.4	15,086.1	39.231
	Total	1,238,741	644,411	10,513.6	1,893,666	
Producer accuracy (%)		92.4	63.6	56.3		OA: 82.42

Table 9 PALSAR-FNF 2020 coverage versus KRDF geodatabase (former extent)

FM 2014 (ha)						
PALSAR-FNF 2020 (ha)		Forest	Non-Forest	Water	Total	User accuracy (%)
	Forest	1,101,999	204,626.1	429.56	1,307,055	84.31
	Non-Forest	131,712.9	435,639.8	4164.83	571,518	76.23
	Water	3662	5512.11	5919.19	15,093.3	39.217
	Total	1,237,374	645,778	10,513.6	1,893,666	
Producer accuracy (%)		89.1	67.5	56.3		OA: 81.51

thought to be resulting from the penetration capability and larger, 25 × 25 m, of L-band SAR ground sampling footprint.

Producer accuracies yielded 89.1% in 2020 and 92.9% in 2017 for forest class, 62.9% in 2018 and 67.5% in 2020 for non-forest class and 56.3% for water class in all years.

When evaluated in general, both dataset's yearly coverages across all years were rather fair in defining the forest class. On the other hand, ESRI land-cover user accuracies produced still very competitive results compared to those of PALSAR-FNFs (Tables 2, 3, 4, 5, 6, 7, 8 and 9).

Visual evaluation

The land-cover datasets used in this research have been prepared worldwide. Positional accuracies of land classes in the research area differ from one another. The main reason for these differences was that these datasets were prepared utilizing different resolution satellite imageries. The boundary differences between forest and non-forest classes can be seen in Fig. 3. As the resolution coarsened, the number of fragmentation increased and can be seen outside the forest boundaries in natural landscapes. On the contrary, the data structure with coarser resolution has reached higher values in accuracy calculations because it covered more area than the specified boundaries. Since the PALSAR datasets was produced using SAR images, more aerial consistency was achieved, but provided less boundary precision.

A 1367.04 ha productive forest area ravaged in a forest fire in Taskopru forest enterprise in September 2020, was deducted from 2020 rectified validation geodatabase (Fig. 2). Although we updated the validation dataset from the validation dataset, no such incident was present in either datasets 2020 coverages (Fig. 2).

Although viewed only as a local visual comparison, when KRDF geodatabase sub-compartment boundaries were overlaid on ESRI coverages, their rather spot-on raster to vector match was noteworthy (Fig. 3). Since Palsar images with low spatial resolution based upon a larger footprint than the control images, they gave better results than those of the ESRI images, computationally. Since the calculations were made on an area basis, both user and manufacturer accuracies were higher than ESRI. However, this situation causes the real borders to appear larger than what they actually were. When viewed from the perspective of borderline reality, ESRI images produced more accurate boundaries.

Discussion

Using a field validation dataset finalized in 2014 against the latter years' 2017–2020, finalized ESRI and PALSAR-FNF coverages might sound strange in the first glance. However, it should be noted that the forests existing in the study region are managed and rotated with 40–60 year cycles for fast growing species (Turkish (Red) pine, Maritime pine) and 100–120 years for other species (Calabrian pine, Scotch pine, Fir, Beech, Chestnut, etc.). Forest management plans are generally renewed in every 10th year. In Turkish forestry practice, one-tenth of all management plans is renewed across the country per year. Thus, even with the shorter rotations, the forest management plans which made up the entire KRDF geodatabase were still sound and reliable enough for the fully stocked study area, because main and sub-compartments have only been tended, preserving

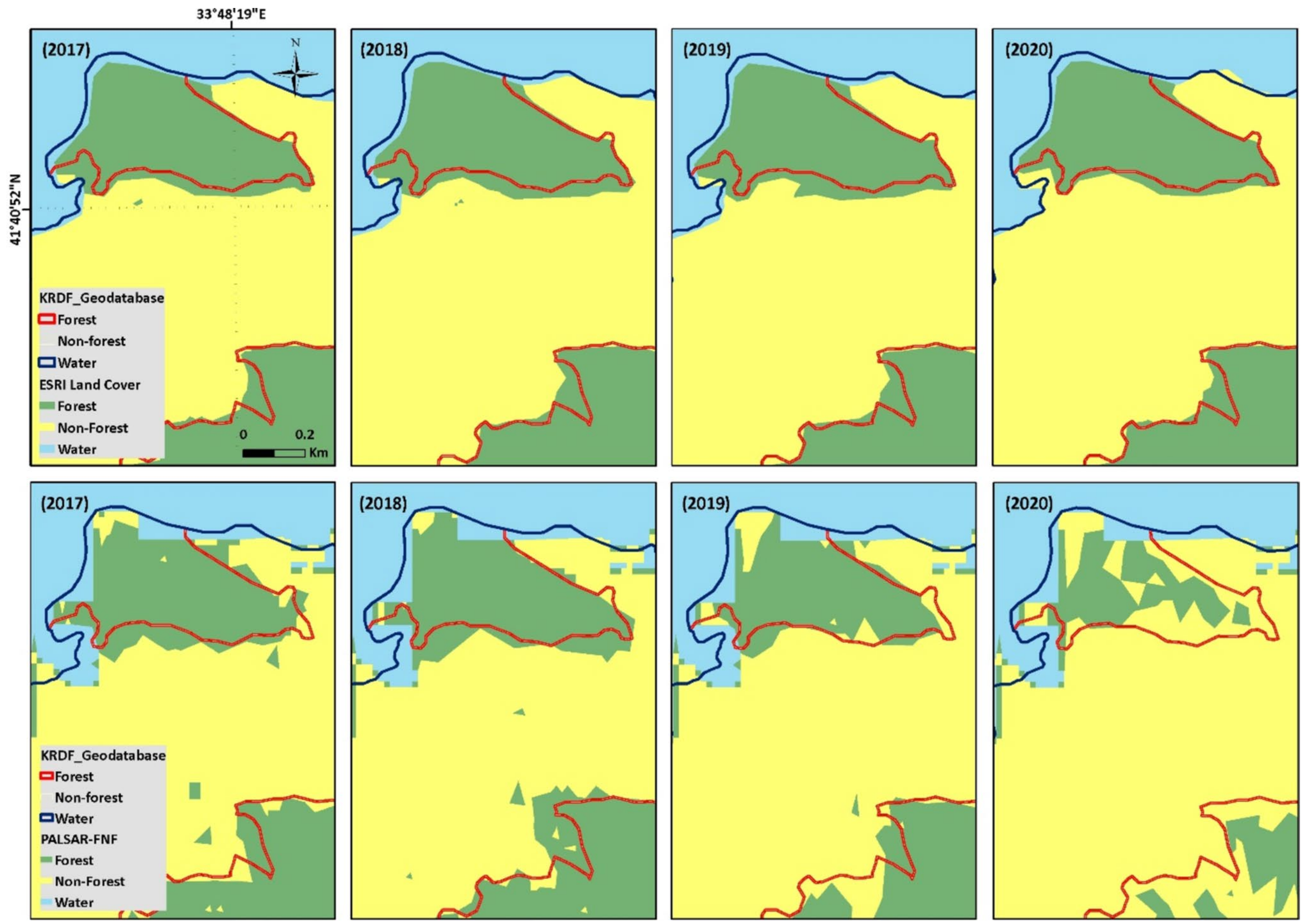

Fig. 3 ESRI Land-cover and PALSAR-FNF year comparisons by validation polygon tracing

a crown-closure. Regeneration works in the study area are carried out according to silvicultural prescriptions, and it is not possible to completely deforest the stands employing natural regeneration methods.

Sentinel-2 s were the next generation newer satellites, supplementary to Landsat-8 for gap filling in the last 2018 coverage of Copernicus CORINE Land-cover (CLC). Karra et al. (2021) found in a similarly fashioned globally scaled Sentinel-2 based land-cover land-use study that an overall accuracy of 85% across ten defined classes was achieved over the designated regions. Although ESRI 9 classes were good in possible detail, there needed to be more validation data in class separation, and the algorithms need to be directed correctly in image analysis. If these errors can be eliminated over time, it will certainly increase the accuracy rate to about 75% worldwide (Venter et al 2022).

Aune-Lundberg and Strand (2021) said CLC-2018 coincided well with the class definitions in general when compared to a detailed national land-cover land use data in Norway, but lacked the same sensitivity in marginal classes. Although we neither had those marginal classes in our study area, nor the reclassification we employed left any, we encountered similar phenomenon in non-forest class where anything, but forests were compiled, when the results were observed while forest class definitions across the years were successful in user accuracies. In comparison, PALSAR-FNF non-forest definitions for 2017, 2018 and 2019 were as satisfactory as those of the forest definitions, except the year 2020 (Tables 6, 7, 8 and 9). Although September 2020 fire in Taskopru was marginal, but perfectly detectable from the space, was missing in both comparison datasets, their forest class definitions were also good slightly favoring ESRI coverages in user accuracies (Tables 2, 3, 4 and 5). Costa et al. (2021) effectively showed the supportive performance of PALSAR-2 SAR imagery over Sentinel-2 based land-cover detection. For simplicity, we consolidated original ESRI land-cover classes focusing on the performance of forest class, and this apparently improved ESRI yearly class definitions as Ma et al. (2020) also mentioned that optical Sentinel images acquired and used to construct that year's coverage made a considerable contribution to the detection of the intended target. When all three classes were considered, either dataset's overall accuracy against the rectified validation geodatabases were above 80% in all years. Compared to Landsat or any other similarly sampled data, Sentinel-2 imagery is nine times better in spatial resolution, as well as in the resulting spectral resolution, however there must still have been some uncertainties in land-cover e.g. unproductive-forest areas, not enough canopy cover, recent land-use change, excessively fragmented land-cover (De Petris et al. 2023), etc., which taint the spectral reflectance in small footprints making a considerable sum at the end, so the end product bears the scars.

Similarly, we found comparably similar results, around 80.47% using our three consolidated classes in ESRI coverages when all years overall accuracies were considered (Tables 2, 3, 4 and 5), whereas PALSAR-FNF coverages managed no less than 82.29% (Tables 6, 7, 8 and 9). The biggest difference between the two comparison datasets was the fact that ERSI coverages were made with optical, while PALSAR ones were made with L-band SAR capabilities. Under favorable conditions e.g. no-cloud, ideal atmospheric conditions, etc. Sentinel-2 images must have produced better recognition compared to L-band SAR operating ALOS images. Li et al. (2022) showed that signal saturation which plagued the 25 m Palsar-2 images caused them to perform worse in an above ground biomass (AGB) calculation study in Japan than Sentinel-2 based ones, but also suggested that the model that combined the two datasets produced the best result in every attempt. Closely, Pham et al. (2020) although mentioned about the same problem, stated that when the two were combined as complementary to one another in a Vietnam study, the resulting AGB calculation was rather satisfactory in the tropics. However, it was remarkable that the success of PALSAR-2 coverages especially in forest class in this study came without the help of any other data (Vatandaslar et al. 2024). Apparently, in predominantly forested and occasional and sporadic urban settings like the study area used in this study, non-forest designation in ESRI land-cover might have somewhat been misclassified due to other consolidated classes within and was therefore not as satisfactorily designated as forest and non-forest (Priem et al. 2019; Qiu et al. 2019).

Altunel et al. (2020) showed while questioning two of PALSAR-FNF coverages, 2007 and 2017, against Landsat based validations calculated in hydroelectric dam reservoirs that although somewhat respectable, they were overly exaggerating the field facts. We did not see any similar tendency in either forest or non-forest classes, water class definitions were rafter flimsy taking the overall success of the database down. It was more than likely from the fact when the large footprint, 25×25 m, of L-band SAR detected a water surface, the percentage of the water inside a pixel was the decisive factor in its class designation in the final product (Gudiyangada Nachappa et al. 2020). Some algorithm-based glitches might have happened during the finalized year coverages. Besides, many study already showed that the longer wavelength of L-band SAR was perfectly capable of penetrating the surface and capturing the soil humidity (Kim et al. 2017; Zribi et al. 2019; Bhogapurapu et al. 2022). Humidity trapped around the water surfaces, possibly registering as an excessive belt around the water bodies, added superficial acreage over the final calculations.

Validation data was obtained from the currently used management plans. When making management plans, rigorous field measurements and supplementarily used orthophotos produced with photogrammetric techniques were used to delineate the boundaries of the forest compartments and composition classes. Validations made by other researchers have stated that accuracy is over 90%, especially on forest border lines (Baskent 2024). As can be seen in Fig. 4, since the validation dataset borders were drawn manually, they fit perfectly in Google earth images. In ESRI land-covers' case, as the resolution increased, the number of fragments increased and started appearing outside the stand borders in natural settings. On the other hand, in PALSAR-FNFs' case, the coarser resolution intrinsically generalized the patches and covered only superficially more area than the actual extend, it indirectly increased the accuracy. Similarly, Palsar land-cover provided more consistent but less boundary sensitive matching owing to lower resolution SAR images.

Conclusion

There appear to be direct and indirect reasons dictating the variations we see in land-cover and land use changes. Forest cover-wise, such changes are directly related to human preferences and climatic variations. However, technology is always improving and becoming a better factor in monitoring the trends and culprits. What we compared in this study was the derived products of two popular datasets, produced using application tested reliable optic and SAR imageries. One of such data that has been the building block of ESRI's land-cover maps, 2017–2021, was SENTINEL-2 imagery. Another similar data using L-band SAR imagery, spanning the same time frame, which has long been in circulation by JAXA, was PALSAR-2/PALSAR/JERS-1 Mosaic and Forest / Non-forest maps. They both were simultaneously run against a detailed land-cover geodatabase in North-central Türkiye to reach to an unbiased result of which would perform better. When accuracy measures were considered, PALSAR-FNF coverages looked better, when overall accuracies were concerned. PALSAR-FNF coverages scored no less than 81.51% in all years whereas ESRI coverages only reached 81% in one year, 2017. However, ESRI coverages' rather successful fit with the questioning parcel boundaries

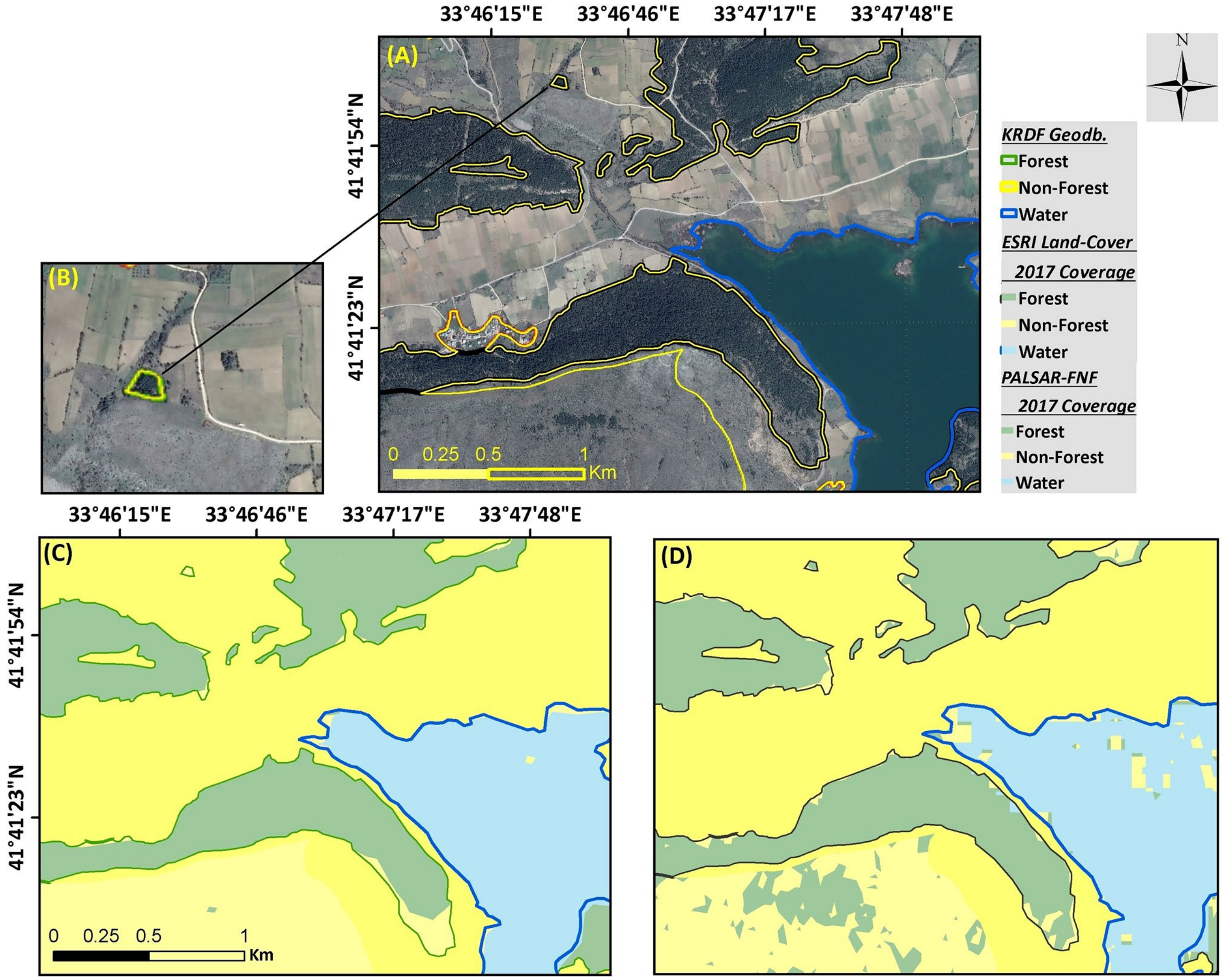

Fig. 4 **A** KRDF geodatabase over current base-map image, **B** a stand within non-forest, KRDF geodatabase on **C** ESRI Land-cover insert and on **D** PALSAR-FNF insert

of the geodatabase was unsurpassed. When PALSAR-FNF results were evaluated, the highest user accuracy with 84.31% was achieved in forest class in 2020. On the contrary, ESRI land-cover produced the highest user accuracy with 87.9% in forest class in 2020. Similarly, PALSAR-FNF produced the highest producer accuracy with 92.9% in forest class in 2017, whereas ESRI land-cover produced the highest producer accuracy with 84% in forest class in 2017.

The use of ESRI's 9-class algorithm in land classification has caused it to show poor performance against a coarse-resolution dataset like PALSAR-FNF, as it provided fragmented data with sharper boundaries at the outer boundary line of forest and non-forest land, however this assumption was not a generalization for other remotely sensed data. The satellite imagery used by ESRI increased the spatial accuracy due to Sentinel-2 s' 10 m spatial resolution. Unfortunately, when the resolution increases, it increases the fragmentation possibility as it starts differentiating the small other spaces within the forests. If those spaces within the forest are eliminated from the year coverages, such fragmentation would not be an issue.

When applied algorithms are further improved, we think the outcomes would be much better nullifying the practicalities of the lower resolution datasets. PALSAR-FNF coverages success was clearly the result of being a purpose oriented dataset with rather limited number of classes, whereas ESRI coverages represented typical land-cover datasets, high accuracy measures have always been hard to achieve with numerous classes.

Land-cover data can make important contributions to forest management policies in Turkey as well as in the rest of the Earth. Such data allows monitoring of critical elements such as the expansion or deterioration of forest cover, the change of tree species and the conservation of biodiversity. Forest areas in Turkey are of great importance, especially for rural development, combating climate change and protecting water resources. Land-cover change analyzes can help identify the trends or problems in these areas. It can be a valuable guide to make forest management policies anywhere in more conscious and sustainable manner. Regional authorities can use these data effectively in policy development processes.

Geographical and climatic conditions should be taken into account when choosing between SAR based or optical data for regional forest management planning in Turkey as well as in the rest of the World. For example, in areas such as the eastern Black Sea region where cloud cover is common, SAR data such as may be more suitable to prevent cloud-induced data loss in optical data. However, in regions with less cloud and more favorable weather conditions, such as the study area, optical imagery based datasets such as ESRI Land-cover may be preferred for more detailed visual analysis and plant health monitoring. Both have advantages and disadvantages, so one is not definitely better than the other one. But this assumption looks to be changing in favor of the optical datasets in the near future.

Leveraging machine learning and optimization techniques such as improved dep/machine learning techniques to improve the classification process in large-scale land-cover mapping projects such as the ESRI datasets can further increase the accuracies and minimize misclassifications. The results were rather similar in terms of which dataset was better performing. SAR advantage over optical data is undeniable but as the data quality and applied methodological approaches are further developed in the upcoming years, optical datasets will certainly match, if not surpass SAR data capabilities.

Both datasets are considerably extensive for both Turkiye and anyplace on Earth. However, they are only good as long as a sound reference possibility is available. Similar validation datasets are present throughout Turkiye, but there are many nations without financial means and capacity to build or acquire such national datasets. In such dire cases, these global datasets can be of great importance monitoring the favorable or undesirable trends happening on a nation's natural resources.

Acknowledgements We thank both ESRI and JAXA for freely disseminating their end-products for everyone to enjoy. We also appreciate the KRDF's and SRDF's involvements in supplying the combined verification dataset.

Author contributions Arif Oguz Altunel conceptualized the study, acquired both ESRI and PALSAR datasets, converted the raster data to vector format for further analyses, and wrote the manuscript. Durmuş Ali Çelik did all spatial questioning and produced the results, corresponding tables, visual aids and edited the methodology.

Funding No funding was obtained for this study.

Data availability Both ESRI and PALSAR data are freely available to the interested parties via https://www.arcgis.com/home/item.html?id=d6642f8a4f6d4685a24ae2dc0c73d4ac and https://www.eorc.jaxa.jp/ALOS/en/palsar_fnf/data/index.htm. Validation dataset access, on the other hand, was given only on grounds of scientific usage, so no sharing is possible.

Declarations

Conflict of interest No conflict of interest was raised by any of the authors or by the supporting agencies.

References

Aksoy H, Kaptan S (2022) Simulation of future forest and land use/cover changes (2019–2039) using the cellular automata-Markov model. Geocarto Int 37(4):1183–1202

Akturk E, Altunel AO, Atesoglu A, Seki M, Erpay S (2023) How good is TanDEM-X 50 m forest/non-forest map? Product validation using temporally corrected geo-browser supplied imagery through collect Earth. Int J Geogr Inf Sci 37(5):1041–1068

Altunel AO, Kara F (2023) Tracing the culprits over the destruction of three coastal communities during a rouge rainstorm on August 2021 in north central Türkiye. Ocean Coast Manag 241:106630

Altunel AO, Akturk E, Altunel T (2020) Examining the PALSAR-2 Global forest/non-forest maps through Turkish afforestation practices. Int J Remote Sens 41(16):6071–6088

Altunel AO (2023) The effect of DEM resolution on topographic wetness index calculation and visualization: an insight to the hidden danger unraveled in Bozkurt in August, 2021. Int J Eng Geosci 8(2):165–172

Altunel AO, Celik DA (2023) Sentinel-2 derivatives are rewriting land-cover history. 6th Advanced Engineering Days (AED), March 5th, 2023, Mersin, Türkiye, pp. 83–85. https://publish.mersin.edu.tr/aed.mersin.edu.tr/wp-content/uploads/2023/07/AED6v3.pdf. Accessed 5 Nov 2024

Atalay I, Efe R (2010) Structural and distributional evaluation of forest ecosystems in Türkiye. J Environ Biol 31(1):61

Aune-Lundberg L, Strand GH (2021) The content and accuracy of the CORINE land-cover dataset for Norway. Int J Appl Earth Obs Geoinf 96:102266

Baskent EZ (2024) A thorough assessment of various forest management planning initiatives and development of improvement strategies towards an ecosystem-based planning. Environ Dev 50:101006

Baskent EZ, Terzioglu S, Baskaya S (2008) Developing and implementing multiple-use forest management planning in Türkiye. Environ Manage 42:37–48

Bharatkar PS, Patel R (2013) Approach to accuracy assessment tor RS image classification techniques. Int J Sci Eng Res 4(12):79–86

Bhogapurapu N, Dey S, Mandal D, Bhattacharya A, Karthikeyan L, McNairn H, Rao YS (2022) Soil moisture retrieval over croplands using dual-pol L-band GRD SAR data. Remote Sens Environ 271:112900

Camalan S, Cui K, Pauca VP, Alqahtani S, Silman M, Chan R, Lutz DA (2022) Change detection of amazonian alluvial gold mining using deep learning and sentinel-2 imagery. Remote Sensing 14(7):1746

Campbell JB (1996) Introduction to Remote Sensing, 2nd edn. Virginia Polytechnic Institute and State University, The Guildford Press, London

Campbell JB, Wynne RH (2011) Introduction to Remote Sensing. Guildford Press, Fifthed, p 667

Cazaubiel V, Chorvalli V, Miesch C (2017) The multispectral instrument of the Sentinel2 program. In: International conference on space optics—ICSO 2008, vol 10566. SPIE, pp 110–115

Celik H, Sengonul K, Akyuz F, Altunel O, Dagci M, Esin A (2012) İstanbul'un içme suyu barajlarının sedimantasyon problemi ve çözüm önerileri: Alibey Barajı örneği. J Fac Forest Istanbul Univ 62(2):113–127

Celik DA, Sahin A (2023) Spatiotemporal changes of carbon storage in Çaltepe Forest Planning Unit. Artvin Çoruh Üniversitesi Orman Fakültesi Dergisi 24(2):224–233

Chen L, Li S, Bai Q, Yang J, Jiang S, Miao Y (2021) Review of image classification algorithms based on convolutional neural networks. Remote Sensing 13(22):4712

Comert R, Matci DK, Avdan U (2019) Object based burned area mapping with random forest algorithm. Int J Eng Geosci 4(2):78–87

Congalton RG (1991) A review of assessing the accuracy of classifications of remotely sensed data. Remote Sens Environ 37(1):35–46

Congalton RG, Green K (2019) Assessing the Accuracy of Remotely Sensed Data: Principles and Practices, Third Edition (3rd ed.). CRC Press. 346.

Costa JDS, Liesenberg V, Schimalski MB, Sousa RVD, Biffi LJ, Gomes AR, Bispo PDC (2021) Benefits of combining ALOS/PALSAR-2 and Sentinel-2A data in the classification of land-cover classes in the Santa Catarina southern Plateau. Remote Sens 13(2):229

De Petris S, Sarvia F, Borgogno-Mondino E (2023) Uncertainty assessment of Sentinel-2-retrieved vegetation spectral indices over Europe. Eur J Remote Sens 101:180

Dibs H, Ali AH, Al-Ansari N, Abed SA (2023a) Fusion Landsat-8 thermal TIRS and OLI datasets for superior monitoring and change detection using remote sensing. Emerg Sci J 7(2):428–444

Dibs H, Jaber HS, Al-Ansari N (2023b) Multi-fusion algorithms for detecting land surface pattern changes using multi-high spatial resolution images and remote sensing analysis. Emerg Sci J 7(4):1215–1231

Galiatsatos N, Donoghue DN, Watt P, Bholanath P, Pickering J, Hansen MC, Mahmood AR (2020) An assessment of global forest change datasets for national forest monitoring and reporting. Remote Sens 12(11):1790

Garcia-Alvarez D, Hinojosa LJ (2022) Global thematic land use cover datasets characterizing vegetation covers. land use cover datasets and validation tools: Validation Practices with QGIS, 373–398.

Garg R, Kumar A, Prateek M, Pandey K, Kumar S (2022) Land-cover classification of spaceborne multifrequency SAR and optical multispectral data using machine learning. Adv Space Res 69(4):1726–1742

Gudiyangada Nachappa T, Kienberger S, Meena SR, Hölbling D, Blaschke T (2020) Comparison and validation of per-pixel and object-based approaches for landslide susceptibility mapping. Geomat Nat Haz Risk 11(1):572–600

Hansen MC, Potapov PV, Moore R, Hancher M, Turubanova SA, Tyukavina A, Thau D, Stehman SV, Goetz SJ, Loveland TR, Kommareddy A, Egorov A, Chini L, Justice CO, Townshend JRG (2013) High-resolution global maps of 21st-century forest cover change. Science 342(6160):850–853. https://doi.org/10.1126/science.1244693

Isaienkov K, Yushchuk M, Khramtsov V, Seliverstov O (2020) Deep learning for regular change detection in Ukrainian forest ecosystem with sentinel-2. IEEE J Sel Topics Appl Earth Obser Remote Sens 14:364–376

Iurist DN, Statescu F, Lateș I (2016) Analysis of land-cover and land use changes using SENTINEL-2 images. Present Environ Sustain Dev 2:161–172

Jiang L, Huang X, Wang F, Liu Y, An P (2018) Method for evaluating ecological vulnerability under climate change based on remote sensing: a case study. Ecol Ind 85:479–486

Kaptan S, Aksoy H, Durkaya B (2022) Estimation of uneven-aged forest stand parameters, crown closure and land use/cover using the Landsat 8 OLI satellite image. Geocarto Int 37(5):1408–1425

Karakus P, Karabork H, Kaya S (2017) A comparison of the classification accuracies in determining the land-cover of Kadirli Region of Türkiye by using the pixel based and object based classification algorithms. Int J Eng Geosci 2(2):52–60

Karra K, Kontgis C, Statman-Weil Z, Mazzariello JC, Mathis M, Brumby SP (2021) Global land use/land-cover with Sentinel 2 and deep learning. In 2021 IEEE international geoscience and remote sensing symposium IGARSS (pp. 4704–4707). IEEE.

Kim SB, Van Zyl JJ, Johnson JT, Moghaddam M, Tsang L, Colliander A, Yueh SH (2017) Surface soil moisture retrieval using the L-band synthetic aperture radar onboard the soil moisture active–passive satellite and evaluation at core validation sites. IEEE Trans Geosci Remote Sens 55(4):1897–1914

Kluczek M, Zagajewski B, Kycko M (2022) Airborne HySpex hyperspectral versus multitemporal Sentinel-2 images for mountain plant communities mapping. Remote Sensing 14(5):1209

Koyama CN, Shimada M, Watanabe M, Tadono T (2022) ALOS-2/PALSAR-2 Long-term Pantropical Observation–A Paradigm Shift in Global Forest Monitoring. In EUSAR 2022; 14th European Conference on Synthetic Aperture Radar (pp. 1–5). VDE.

Kucsicsa G, Balteanu D (2020) The influence of man-induced land-use change on the upper forest limit in the Romanian Carpathians. Eur J Forest Res 139(6):893–914

Kwan C, Budavari B, Bovik AC, Marchisio G (2017) Blind quality assessment of fused worldview-3 images by using the combinations of pansharpening and hypersharpening paradigms. IEEE Geosci Remote Sens Lett 14(10):1835–1839

Lambert MJ, Traoré PCS, Blaes X, Baret P, Defourny P (2018) Estimating smallholder crops production at village level from Sentinel-2 time series in Mali's cotton belt. Remote Sens Environ 216:647–657

Leenstra M, Marcos D, Bovolo F, Tuia D (2021) Self-supervised pre-training enhances change detectionin Sentinel-2 imagery. In Pattern Recognition. ICPR International Workshops and Challenges: Virtual Event, January 10–15, 2021, Proceedings, Part VII (pp. 578–590). Springer International Publishing.

Li H, Kato T, Hayashi M, Wu L (2022) Estimation of forest aboveground biomass of two major conifers in Ibaraki Prefecture, Japan, from palsar-2 and sentinel-2 data. Remote Sensing 14(3):468

Liping C, Yujun S, Saeed S (2018) Monitoring and predicting land use and land-cover changes using remote sensing and GIS techniquesa case study of a hilly area, Jiangle. China Plos One 13(7):e0200493

Lopez JMR, Heider K, Scheffran J (2017) Frontiers of urbanization: Identifying and explaining urbanization hot spots in the south of Mexico City using human and remote sensing. Appl Geogr 79:1–10

Loran C, Kienast F, Bürgi M (2018) Change and persistence: exploring the driving forces of long-term forest cover dynamics in the Swiss lowlands. Eur J Forest Res 137:693–706

Lulla K, Nellis MD, Rundquist B, Srivastava PK, Szabo S (2021) Mission to earth: LANDSAT 9 will continue to view the world. Geocarto Int 36(20):2261–2263

Ma L, Schmitt M, Zhu X (2020) Uncertainty analysis of object-based land-cover classification using Sentinel-2 time-series data. Remote Sens 12(22):3798

Main-Korn M, Pflug B, Louis J, Debaecker V, Müller-Wilm U, Gascon F (2017) Sen2Cor for sentinel-2. in image and signal processing for remote sensing XXIII. SPIE 10427:37–48

Nkeumoe Numbisi F, Vancoillie F, De Wulf R (2018) Multi-date sentinel1 SAR image textures discriminate perennial agroforests in a tropical forest-savannah transition landscape. In Mid-term symposium'Innovative sensing: from sensors to methods and applications' (Vol. 42, pp. 339–346). Copernicus Gesellschaft.

Ohki M, Tadono T, Itoh T, Ishii K, Yamanokuchi T, Watanabe M, Shimada M (2019) Flood area detection using PALSAR-2 amplitude and coherence data: the case of the 2015 heavy rainfall in Japan. IEEE J Sel Top Appl Earth Obs Remote Sens 12(7):2288–2298

Pastick NJ, Wylie BK, Wu Z (2018) Spatiotemporal analysis of Landsat-8 and Sentinel-2 data to support monitoring of dryland ecosystems. Remote Sensing 10(5):791

Pham TD, Le NN, Ha NT, Nguyen LV, Xia J, Yokoya N, Takeuchi W (2020) Estimating mangrove above-ground biomass using extreme gradient boosting decision trees algorithm with fused sentinel-2 and ALOS-2 PALSAR-2 data in can Gio biosphere reserve. Vietnam Remote Sens 12(5):777

Phiri D, Simwanda M, Salekin S, Nyirenda VR, Murayama Y, Ranagalage M (2020) Sentinel-2 data for land-cover/use mapping: a review. Remote Sensing 12(14):2291

Priem F, Okujeni A, van der Linden S, Canters F (2019) Comparing map-based and library-based training approaches for urban land-cover fraction mapping from Sentinel-2 imagery. Int J Appl Earth Obs Geoinf 78:295–305

Qiu C, Mou L, Schmitt M, Zhu XX (2019) Local climate zone-based urban land-cover classification from multi-seasonal Sentinel-2 images with a recurrent residual network. ISPRS J Photogramm Remote Sens 154:151–162

Rouse JW, Haas RH, Scheel JA, Deering DW (1974) Monitoring Vegetation Systems in the Great Plains with ERTS. In: Proceedings, 3rd Earth Resource Technology Satellite (ERTS) Symposium, 1 48–62.

Roy DP, Huang H, Boschetti L, Giglio L, Yan L, Zhang HH, Li Z (2019) Landsat-8 and Sentinel-2 burned area mapping-a combined sensor multi-temporal change detection approach. Remote Sens Environ 231:111254

Shimada M, Itoh T, Motooka T, Watanabe M, Shiraishi T, Thapa R, Lucas R (2014) New global forest/non-forest maps from ALOS PALSAR data (2007–2010). Remote Sens Environ 155:13–31

Skalos J, Engstova B, Trpakova I, Santruckova M, Podrazsky V (2012) Long-term changes in forest cover 1780–2007 in central Bohemia, Czech Republic. Eur J Forest Res 131:871–884

Stehman SV, Foody GM (2019) Key issues in rigorous accuracy assessment of land-cover products. Remote Sens Environ 231:111199

Townshend JR, Masek JG, Huang C, Vermote EF, Gao F, Channan S, Sexton JO, Feng M, Narasimhan R, Kim D-H, Song K, Song D, Song X, Noojipady P, Tan B, Hansen MC, Li M, Wolfe R (2012) Global characterization and monitoring of forest cover using Landsat data: opportunities and challenges. Int J Digital Earth 5:373–397

URL-1. (2023). ESRI land-cover. Available through https://www.arcgis.com/home/item.html?id=d6642f8a4f6d4685a24ae2dc0c73d4ac, last accessed in 13.10.2024.

URL-2 (2023) Global 25 m Resolution PALSAR Mosaic and Forest/Non-Forest Map (FNF).Available through https://www.eorc.jaxa.jp/ALOS/en/palsar_fnf/data/index.htm, last accessed in 13/10/2024.

URL-3 (2017) Ekosistem tabanli fonksiyonel orman amenajman planlarinin duzenlenmesine ait usul ve esaslar, Notification # 299. Available through https://www.ogm.gov.tr/tr/e-kutuphane-sitesi/mevzuat-sitesi/Tebligler/Ekosistem%20Tabanl%C4%B1%20Fonksiyonel%20Orman%20Amenajman%20Planlar%C4%B1n%C4%B1n%20D%C3%BCzenlenmesine%20Ait%20Usul%20ve%20Esaslar.pdf, last accessed in 13/10/2024.

URL-4 (2019) Criteria and Indicators of Sustainable Forest Management. General Directorate of Forestry, Implementation Guide. Available through https://www.ogm.gov.tr/tr/e-kutuphane-sitesi/SurdurulebilirOrmanYonetimi/SFM%20C-I%20IMPLEMENTATION%20GUIDE.pdf, last accessed in 13/10/2024.

Vatandaslar C, Bolat F, Abdikan S, Pamukcu-Albers P, Satiral C (2024) Modeling aboveground carbon in flooded forests using synthetic aperture radar data: a case study from a natural reserve in Turkish Thrace. iForest-Biogeosciences and Forestry 17(5):277

Vaz AS, Gonçalves JF, Pereira P, Santarém F, Vicente JR, Honrado JP (2019) Earth observation and social media: evaluating the spatiotemporal contribution of non-native trees to cultural ecosystem services. Remote Sens Environ 230:111193

Venter ZS, Barton DN, Chakraborty T, Simensen T, Singh G (2022) Global 10 m land use land-cover datasets: a comparison of dynamic world, world cover and ESRI land-cover. Remote Sens 14(16):4101

Wang R, Wu K, He Q, He Y, Gu Y, Wu S (2022) A novel method of monitoring surface subsidence law based on probability integral model combined with active and passive remote sensing data. Remote Sensing 14(2):299

Watanabe M, Thapa RB, Ohsumi T, Fujiwara H, Yonezawa C, Tomii N, Suzuki S (2016) Detection of damaged urban areas using interferometric SAR coherence change with PALSAR-2. Earth, Planets and Space 68(1):1–12

Wulder MA, Masek JG (2012) Landsat legacy. Remote Sens Environ 122:1

Zhang P, Ke Y, Zhang Z, Wang M, Li P, Zhang S (2018) Urban land use and land-cover classification using novel deep learning models based on high spatial resolution satellite imagery. Sensors 18(11):3717

Zhu Q, Guo X, Deng W, Shi S, Guan Q, Zhong Y, Li D (2022) Land-use/land-cover change detection based on a Siamese global learning framework for high spatial resolution remote sensing imagery. ISPRS J Photogramm Remote Sens 184:63–78

Zribi M, Muddu S, Bousbih S, Al Bitar A, Tomer SK, Baghdadi N, Bandyopadhyay S (2019) Analysis of L-band SAR data for soil moisture estimations over agricultural areas in the tropics. Remote Sensing 11(9):1122